

Supramolecular Assemblies Involving Organometallic Free Acids

Timothy E. Baroni,[†] Joseph A. Heppert,^{*,†} Rolande R. Hodel,[†]
Richard P. Kingsborough,[‡] Martha D. Morton,[†] Arnold L. Rheingold,^{*,§} and
Glenn P. A. Yap[§]

Department of Chemistry, University of Kansas, Lawrence, Kansas 66045, and Department of
Chemistry and Biochemistry, University of Delaware, Newark, Delaware 19716

Received May 14, 1996[⊗]

Reactions between $W(\eta^2\text{-Ph}_2\text{C}_2)\text{Cl}_4$ and salicylic acid derivatives generate analytically pure free acids of formula $W(\eta^2\text{-Ph}_2\text{C}_2)\text{Cl}_3(\text{Hsal-R})$ (**1**) in high yields (Hsal = a salicylate monoanion). The products exist as hydrogen-bonded dimers in the solid state. The acid functionality on one molecule hydrogen bonds to one of the *cis*-chloride ligands of an adjacent complex at a 3.03 Å distance. The more electron-rich tungsten center renders these acetylene complexes less acidic than their oxo and arylimido analogs. As a result, $W(\eta^2\text{-Ph}_2\text{C}_2)\text{Cl}_3(\text{Hsal})$ exhibits partial dimerization in solution and have relatively weak hydrogen bonds to nitrogen- and oxygen-containing organic molecules. Among a range of possible phenol–phenoxide complexes of the $W(\eta^2\text{-Ph}_2\text{C}_2)\text{Cl}_3$ subunit, only the ether adduct of the catecholate, $W(\eta^2\text{-Ph}_2\text{C}_2)\text{Cl}_3(\text{Hcat}\text{-OEt}_2)$ (**2**), has been isolated and structurally characterized. The weaker hydrogen bond strength of larger chelating bis(phenolates) evidently destabilize the phenol–phenoxide structures in favor of simple chelating bis(phenoxides). The salicylate free acids form various supramolecular complexes in solution and the solid state, including $[W(\eta^2\text{-Ph}_2\text{C}_2)\text{Cl}_3(\text{Hsal})]_4(18\text{-crown-6})$ (**5**), one of a family of tetranuclear systems organized around hydrogen bonding to an 18-crown-6 template. This structure is characterized by π -stacking of the Hsal ligands between confacial free acid complexes and the steric screening of the two non-hydrogen-bonded 18-crown-6 oxygens by pairs of antarafacial $W(\text{Ph}_2\text{C}_2)$ units.

Introduction

From their inception, strategies for the assembly of supramolecular molecules and materials have relied on hydrogen-bonding interactions as critical organization elements.^{1–7} The use of these functional groups as building blocks follows naturally from the critical structural and reactive role that they play in functional biological supramolecular systems.^{8–10} Today, a broad range of synthetic supramolecular species employ organizationally and chemically functional hydrogen bonds that either have been introduced serendipitously or have been carefully woven into the design of molecular

subunits.^{11–19} Supramolecular species containing hydrogen bonds have found a variety of applications in biomimicry as receptors and switches and in materials applications ranging from catalysis to photonic materials.^{20,21} Recently, numerous structural and thermodynamic studies have focused on transition metal complexes containing both intramolecular and intermolecular hydrogen-bonding interactions.^{22–26} Some projects have sought to understand the kinetics and thermodynamics

* Authors to whom correspondence should be addressed.

[†] University of Kansas.

[‡] NSF-URP student from the University of Arizona. Current address: Department of Chemistry, University of Pennsylvania, Philadelphia, PA 19104.

[§] University of Delaware.

[⊗] Abstract published in *Advance ACS Abstracts*, September 15, 1996.

(1) Balzani, V.; DeCola, L., Eds. *Supramolecular Chemistry*; NATO-ASI; Kluwer Academic Publishers: Dordrecht, The Netherlands, 1992.

(2) Sutherland, I. O., Ed. *Host-Guest Molecular Interactions: From Chemistry to Biology*; J. Wiley and Sons: New York, 1991.

(3) Cram, D. J.; Cram, J. M. *Container Molecules and Their Guests*; The Royal Society of Chemistry: Cambridge, United Kingdom, 1994.

(4) Desiraju, G. R. *Angew. Chem., Int. Ed. Engl.* **1995**, *34*, 2311.

(5) Aakeröy, C. B.; Seddon, K. R. *J. Chem. Soc. Rev.* **1993**, 397.

(6) Aakeröy, C. B.; Nieuwenhuysen, M. *J. Mol. Struct.* **1996**, *374*, 223.

(7) Russell, V. A.; Etter, M. C.; Ward, M. D. *J. Am. Chem. Soc.* **1994**, *116*, 1941.

(8) Pifat-Mrzljak, G., Ed. *Supramolecular Structure and Function*; World Scientific Publishing Co.: Singapore, 1988.

(9) Friedrich, P. *Supramolecular Enzyme Organization*; Pergamon Press: Oxford, United Kingdom, 1984.

(10) Kiefer, L. L.; Paterno, S. A.; Fierke, C. A. *J. Am. Chem. Soc.* **1995**, *117*, 6831.

(11) Mathias, J. P.; Seto, C. T.; Simanek, E. E.; Whitesides, G. M. *J. Am. Chem. Soc.* **1994**, *116*, 1725–1736.

(12) Schall, O. F.; Gokel, G. W. *J. Am. Chem. Soc.* **1994**, *116*, 6084–6100.

(13) Prasad, P. N.; Reinhardt, B. A. *Chem. Mater.* **1990**, *2*, 660–669.

(14) Wilcox, C. S.; Adrian, J. C.; Webb, T. H.; Zawaeki, F. J. *J. Am. Chem. Soc.* **1992**, *114*, 10189.

(15) Král, V.; Furuta, H.; Shreder, K.; Lynch, V.; Sessler, J. L. *J. Am. Chem. Soc.* **1996**, *118*, 1595.

(16) Hamilton, A. D.; Goodman, M. S.; Weiss, J. *J. Am. Chem. Soc.* **1995**, *117*, 8447.

(17) Valdés, C.; Spitz, V. P.; Toledo, L. M.; Kubik, S. W.; Rebek, T. *J. Am. Chem. Soc.* **1995**, *117*, 12733.

(18) Lynch, D. E.; Smith, G.; Freney, D.; Byriel, K. A.; Kennard, C. H. L. *Aust. J. Chem.* **1994**, *47*, 1097.

(19) Manabe, K.; Okamura, K.; Date, T.; Koga, K. *J. Org. Chem.* **1993**, *58*, 6692.

(20) Tsao, B. L.; Pieters, R. J.; Rebek, J. *J. Am. Chem. Soc.* **1995**, *117*, 2210.

(21) Christe, S. D.; Subramanian, S.; Thompson, L. K.; Zaworotko, M. J. *J. Chem. Soc., Chem. Commun.* **1994**, 2563.

(22) (a) Griffith, W. P.; Noguera, H. I. S.; Parkin, B. C.; Sheppard, R. N.; White, A. J. P.; Williams, D. P. *J. Chem. Soc., Dalton Trans.* **1995**, 1775. (b) Simpson, R. D.; Bergman, R. G. *Organometallics* **1993**, *12*, 781. (c) Dervisi, A.; Grove, D. M.; Kooijman, H.; van Koten, G.; Lakin, M. T.; Spek, A. L. *J. Am. Chem. Soc.* **1995**, *117*, 10939.

(23) Griffith, W. P.; Edwards, C. F.; White, A. J. P.; Williams, D. J. *J. Chem. Soc., Dalton Trans.* **1993**, 3813.

(24) Lehtonen, A.; Sillanpää, R. *Polyhedron* **1995**, *14*, 1831.

(25) Kabanos, T. A.; Keramidis, A. D.; Papaicannou, A.; Terzis, A. *Inorg. Chem.* **1994**, *33*, 845.

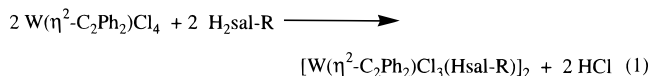
of hydrogen bonding between organic hydrogen bond donors and the basic heteroatoms in the coordination sphere of the complexes. Many investigations have studied the interaction of hydrogen bonding functionality in the metal coordination sphere with complementary sites on organic substrates and other coordination complexes, employing the complexes as a type of simple molecular receptor.^{23–25} An increasing number of researchers have employed hydrogen-bonding metal complexes as components of solid-phase materials.^{11,12,26–28,30–34} Some initial studies have centered on the structural chemistry of metal complexes bearing hydrogen-bonding groups.^{26–34} These systems often adopt organizational motifs homologous with the parent organic functionality. More recently, investigators intent on generating novel two- and three-dimensional materials networks have employed hydrogen-bonding complexes to address specific problems in molecular and crystal engineering.^{35–39}

Our interests in metal-mediated hydrogen-bonding interactions began with the inadvertent discovery of several members of a now extensive class of chelating phenol–phenolate Brønsted acids of tungsten oxo and arylimido complexes.^{40–43} It became clear that these complexes were unique both in the accessibility of a broad range of isoelectronic, isostructural analogs of the tungsten template and in the variability of the hydrogen bond strength of the Brønsted acid. Our long term goal in this project is to utilize the control of hydrogen bond strength available in this class of molecules in the rational assembly of inorganic/organic hybrid materials. In the near term, understanding the structures and association modes of the parent functionality and examining how systematic variations in the metal's electronic environment influence the hydrogen-bonding characteristics of the complexes is central to this objective. We report here the preparation and characteriza-

tion of an uncommon class of d² organometallic free acids of tungsten, W(η^2 -Ph₂C₂)Cl₃(Hsal-R) (**1**), where Hsal-R is a substituted salicylate monoanion. We have found that these complexes can adopt unusual structural motifs in the solid state and form polynuclear aggregates with hydrogen bond acceptor molecules, including some unusually weak Brønsted bases.

Results and Discussion

Synthesis of Salicylate Derivatives of d² Tungsten Acetylene Complexes. Reactions of substituted salicylic acids (H₂sal-R) with W(η^2 -Ph₂C₂)Cl₄⁴⁴ in dichloromethane result in deep red-orange solutions from which high yields of red complexes of formula W(η^2 -Ph₂C₂)Cl₃(Hsal-R) (**1**) are isolated (eq 1). The products



are modestly moisture sensitive, persisting on contact with air in the solid state for up to several weeks and for brief periods in solution. Although other examples of organometallic early transition metal complexes containing hydrogen-bonding ligands are known,^{45,46} these acetylene complexes are unusual, because the tungsten is in a high formal oxidation state, the hydrogen-bonding functionality possesses a low pK_a, and the organometallic functional group is prone to protonolysis. d² tungsten diphenylacetylene complexes hydrolyze to produce stilbenes in protic media.^{40,47} Molecular weights of the analytically pure free acids **1** in benzene solution are determined (by the Signer method⁴⁸) to be between the mono- and dinuclear forms. This is in sharp contrast to the oxo free acid analogs which exist only as dimers in benzene solution.⁴⁰ The d² tungsten centers of the alkyne complexes, which are more electron rich than those in isoelectronic d⁰ oxo complexes, demand less electron density from the carboxylate moiety. This results in reduced hydrogen bond strength in the acid functionality. Both spectroscopic studies and titrations of the isoelectronic tungsten salicylate complexes suggest that the chemistry of the d² tungsten acetylene fragment is more similar to d⁰ tungsten fragments bearing the stronger π -donor (2,6-dimethyl-aryl)imido unit. This trend is not as evident in correlations between aromatic substituent effects (Hammett σ) of groups bound to the Hsal ligand and the carboxylate carbon chemical shift.⁴⁹ Note that the oxo and arylimido compounds have similar " ρ " values, thus showing similar characteristics in their π -donating ability (Figure 1). By comparison, the slope of the Ph₂C₂ complexes is greater due to the reduced electrophilicity of the d² tungsten center. This indicates that the acetylene derivatives are more sensitive to negative charge buildup at the acid group than analogous oxo and arylimido complexes.

(26) Glowiak, T.; Kozlowski, H.; Erre, L. S.; Miora, G.; Gulinati, B. *Inorg. Chim. Acta* **1992**, *202*, 43.

(27) Anson, C. E.; Creaser, C. S.; Stephenson, G. R. *J. Chem. Soc., Chem. Commun.* **1994**, 2175.

(28) Houlton, A.; Mingos, D. M. P.; Williams, D. J. *J. Chem. Soc., Chem. Commun.* **1994**, 503.

(29) Richmond, T. G. *Coord. Chem. Rev.* **1990**, *105*, 221.

(30) Bein, T. *Supramolecular Architecture: Synthetic Control in Thin Films and Solids*; ACS Symposium Series; American Chemical Society: Washington, DC, 1992.

(31) Alsters, P. L.; Baesjou, P. J.; Janssen, M. D.; Kooijman, H.; Sicherer-Roetman, A.; Spek, A. L.; van Koten, G. *Organometallics* **1992**, *11*, 4124.

(32) Kabanos, T. A.; Deramidas, A. D.; Papaioannou, A.; Terzis, A. *Inorg. Chem.* **1994**, *33*, 845.

(33) Braga, D.; Grepioni, F.; Sabatino, P.; Desiraju, G. R. *Organometallics* **1994**, *13*, 3532.

(34) Copp, S. B.; Subramanian, S.; Zaworotko, M. J. *Am. Chem. Soc.* **1992**, *114*, 8719.

(35) Subramanian, S.; Zaworotko, M. J. *Coord. Chem. Rev.* **1994**, *137*, 357.

(36) Zerkowski, J. A.; Mathias, J. P.; Whitesides, G. M. *J. Am. Chem. Soc.* **1994**, *116*, 4305.

(37) Zerkowski, J. A.; Whitesides, G. M. *J. Am. Chem. Soc.* **1994**, *116*, 4298.

(38) Elaiwi, A.; Hitchcock, P. B.; Seddon, K. R.; Srinivasan, N.; Tan, Y.; Welton, T.; Zora, J. A. *J. Chem. Soc., Dalton Trans.* **1995**, 3467.

(39) Kickham, J. E.; Loeb, S. J. *Inorg. Chem.* **1995**, *34*, 5656.

(40) Morton, M. D.; Heppert, J. A.; Dietz, S. D.; Huang, W. H.; Ellis, D. A.; Grant, T. A.; Eilerts, N. W.; Barnes, D. L.; Takusagawa, F.; VanderVelde, D. J. *Am. Chem. Soc.* **1993**, *115*, 7916.

(41) (a) Baroni, T. E.; Heppert, J. A.; Kolesnichenko, V.; Rheingold, A. L.; Yap, G. P. A. Manuscript submitted for publication. (b) Baroni, T. E.; Hodel, R. R.; Heppert, J. A.; Morton, M. D.; Takusagawa, F. Manuscript in preparation.

(42) Person, C.; Oskarsson, A.; Andersson, C. *Polyhedron* **1992**, *16*, 2039.

(43) Bell, A. J. *Mol. Catal.* **1991**, *76*, 165.

(44) Theopold, K. H.; Holmes, S. J.; Schrock, R. R. *Angew. Chem., Int. Ed. Engl.* **1983**, *22*, 1010.

(45) Mazzanati, M.; Floriani, C.; Chiesi-Villa, A. *J. Chem. Soc., Dalton Trans.* **1989**, 1793.

(46) Lehtonen, A.; Sillanpää, R. *J. Chem. Soc., Dalton Trans.* **1994**, 2119.

(47) Nielson, A. J.; Boyd, P. D.; Clark, G. R.; Hunt, T. A.; Metson, J. B.; Richard, C. E. F.; Schwerdtfeger, P. *Polyhedron* **1992**, *11*, 1419.

(48) Clark, E. P. *Ind. Eng. Chem., Anal. Ed.* **1941**, *13*, 820

(49) Hammett, L. P. *Physical Organic Chemistry*; McGraw Hill Book Co.: New York, 1970.

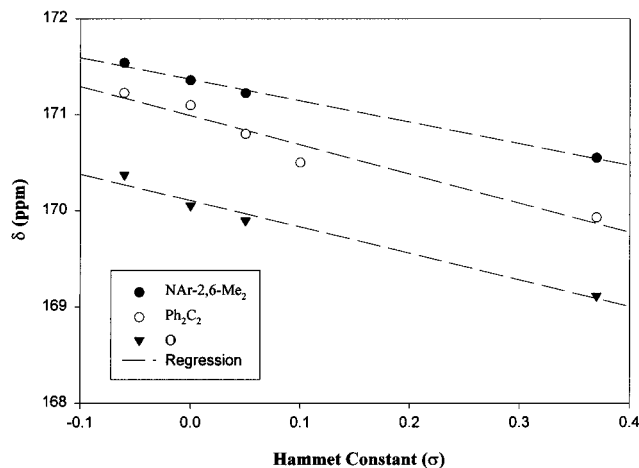
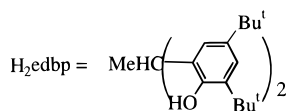
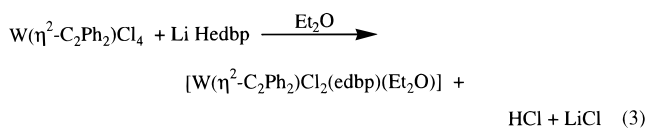
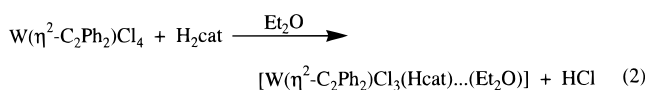


Figure 1. Hammett plot of ^{13}C NMR chemical shifts of Hsal-R carboxylate groups in $\text{W}(=\text{O})\text{Cl}_3(\text{Hsal-R})$, $\text{W}(=\text{NC}_6\text{H}_3-2,6\text{-Me}_2)\text{Cl}_3(\text{Hsal-R})$, and $\text{W}(\eta^2\text{-Ph}_2\text{C}_2)\text{Cl}_3(\text{Hsal-R})$.

Attempts to isolate phenol-phenoxide chelates of the d^2 tungsten acetylene template analogous to those observed for tungsten oxo and imido complexes are complicated by the decreased electrophilicity of the metal. Only $\text{W}(\eta^2\text{-Ph}_2\text{C}_2)\text{Cl}_3(\text{Hcat}\cdots\text{OEt}_2)$ (**2**) ($\text{Hcat} = [\text{o-C}_6\text{H}_4(\text{OH})(\text{O})]^-$) is readily isolated as a diethyl ether adduct (eq 2). We have noted previously in the oxo and



imido cases that the strength of the hydrogen bond to ether decreases as the ring size of the phenol-phenoxide chelating ligand increases.⁴⁰ This leaves complexes with seven- or eight-membered chelate rings more prone to eliminate HCl and produce $\text{W}(=\text{X})\text{Cl}_2(\text{O}-\text{Ar}-\text{O})(\text{L})$ derivatives.^{40,43} In tungsten acetylene complexes, this effect is sufficiently pronounced that bis(phenols) larger than the catechol only produce $\text{W}(=\text{X})\text{Cl}_2(\text{O}-\text{Ar}-\text{O})(\text{L})$ (**3**) species at ambient temperature (eq 3).

Although the origin of this difference in reactivity is unclear, it may result from a combination of the decreasing conformational compatibility of larger bis(phenols) with the tungsten coordination environment and the increased *trans*-effect of the $\eta^2\text{-Ph}_2\text{C}_2$ ligand. The increasing *trans*-influence of the acetylene ligand ($\text{O} < \text{NAr} < \text{Ph}_2\text{C}_2$) will result in greater lability of the *trans*-phenol group. Since the larger ring size chelates already exhibit reduced hydrogen bond strength, the phenol functional group is protected neither by a strong hydrogen bond to ether nor by tenacious coordination to tungsten. These factors appear to greatly increase the rate of proton transfer and HCl elimination from complexes containing seven- and eight-membered phenol-phenoxide chelates.

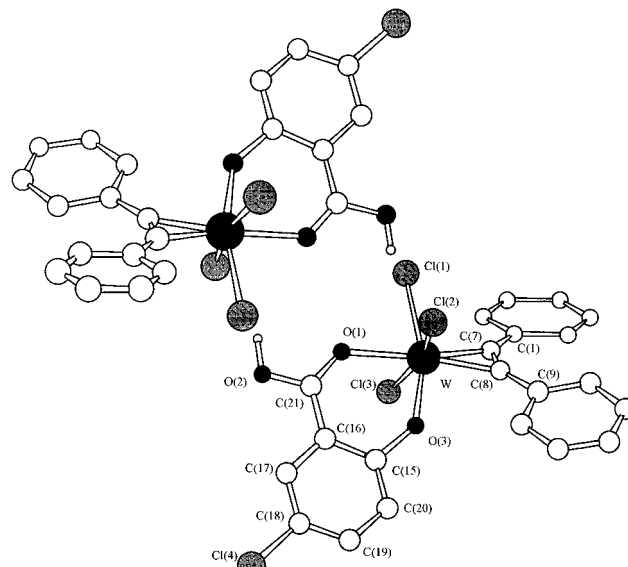
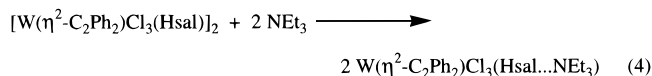


Figure 2. Ball and stick representation of the molecular structure of $[\text{W}(\eta^2\text{-Ph}_2\text{C}_2)\text{Cl}_3(\text{Hsal-5-Cl})]_2$ (**1b**).

Like other organic carboxylates,^{50–52} the spectroscopic and chemical characteristics of interactions between the tungsten free acids and hydrogen bond acceptor molecules (including ethers, amines, and aldehydes) indicate that hydrogen bonding to **1** is weak, even in nonpolar media. While NMR titrations of **1** with ether and oxygen-containing acceptor molecules indicate that Brønsted acid–base adducts are formed, it is difficult to isolate such complexes from solvents other than the neat acceptor molecule. Moreover, once ether adducts are isolated, they are prone to ether loss even in the solid state. The relatively strong self-association of the free acids seems to detract from their ability to bind some classical hydrogen bond acceptors.

This reduction in hydrogen-bonding aptitude can be overcome by several strategies. The triethylammonium salts $\text{W}(\eta^2\text{-Ph}_2\text{C}_2)\text{Cl}_3(\text{sal-R}\cdots\text{HNEt}_3)$ (**4**), which are presumably stabilized by the partial ionic character of the $\text{O}\cdots\text{H}-\text{N}$ interaction, are readily isolated as stoichiometric adducts (eq 4). These “salts” are highly soluble



in benzene, toluene, dichloromethane, and chloroform, indicating that ion pairing minimizes ionic character. Still, the ammonium ions exchange rapidly in solution, as indicated by the presence of broad trialkylammonium proton resonances in ^1H NMR spectra. More insipid hydrogen bonds to organic ethers can be isolated even from dilute solution, providing that higher molecular weight poly(ether)s are employed. This strategy was used in the preparation supramolecular complexes like the $[\text{W}(\eta^2\text{-Ph}_2\text{C}_2)\text{Cl}_3(\text{Hsal})\cdots]_4(18\text{-crown-6})$ (**5**) complex, whose structure is outlined below.

Structures of Representative Brønsted Acid Complexes. The structures of three Brønsted acidic tungsten acetylene derivatives are shown in the ball and stick models in Figures 2–4. Tables 1–3 contain the

(50) Connors, K. A. *Binding Constants*; John Wiley and Sons: New York, 1987.

(51) Grunwald, E.; Price, E. *J. Am. Chem. Soc.* **1964**, *86*, 2965.

(52) Deiter, D. F.; Novak, R. W. *J. Am. Chem. Soc.* **1970**, *92*, 1361.

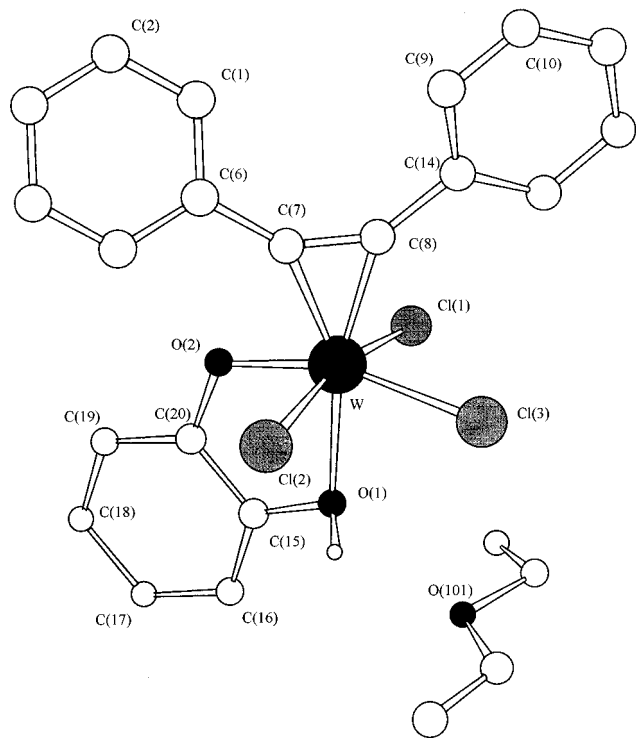


Figure 3. Ball and stick representation of the molecular structure of $[W(\eta^2\text{-Ph}_2\text{C}_2)\text{Cl}_3(\text{Hcat}\cdots\text{OEt}_2)]$ (**2**).

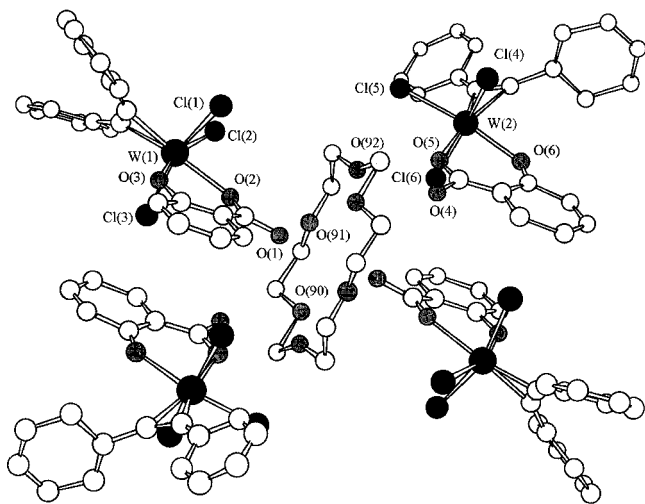


Figure 4. Ball and stick representation of the molecular structure of $[W(\eta^2\text{-Ph}_2\text{C}_2)\text{Cl}_3(\text{Hsal})]_4(18\text{-crown-6})$ (**5**).

pertinent bond distances and angles for these complexes. $W(\eta^2\text{-Ph}_2\text{C}_2)\text{Cl}_3(\text{Hsal-5-Cl})$ (**1b**) and $[W(\eta^2\text{-Ph}_2\text{C}_2)\text{Cl}_3(\text{Hsal})\cdots]_4(18\text{-crown-6})$ (**5**) have a common chelating salicylate monoanion unit, while $W(\eta^2\text{-Ph}_2\text{C}_2)\text{Cl}_3(\text{Hcat}\cdots\text{OEt}_2)$ (**2**) contains the catecholate monoanion. The core $W(\eta^2\text{-Ph}_2\text{C}_2)$ fragment shows similar structural characteristics in all of these complexes. The $W\text{-C}\equiv\text{C}$ and $\text{C}\equiv\text{C}$ distances of **1b** and **2** are very similar, averaging 2.010(10) and 1.318(15) Å, respectively. These distances are characteristic of the $W(\eta^2\text{-Ph}_2\text{C}_2)\text{Cl}_4$ precursor and other d^2 tungsten and molybdenum acetylene derivatives bearing halogen and aryloxy ligands.^{53–61} The $W\text{-C}\equiv\text{C}$ and $\text{C}\equiv\text{C}$ bond lengths found in **5**—2.031(24) and 1.238(31) Å, respectively—initially

(53) Walborsky, E. C.; Wigley, D. E.; Rowland, E.; Dewan, J. C.; Schrock, R. R. *Inorg. Chem.* **1987**, *26*, 1615.

(54) Kriley, C. E.; Kerschner, J. L.; Fanwick, P. E.; Rothwell, I. P. *Organometallics* **1993**, *12*, 2051.

Table 1. Pertinent Bond Lengths (Å) and Angles (deg) for $[W(\eta^2\text{-C}_2\text{Ph}_2)\text{Cl}_3(\text{Hsal-5-Cl})]_2$

W–O(1)	2.211(6)	W–O(3)	1.928(6)
W–Cl(1)	2.339(2)	W–Cl(2)	2.352(3)
W–Cl(3)	2.391(3)	W–C(7)	2.008(9)
W–C(8)	2.019(9)	O(1)–C(21)	1.233(12)
O(2)–C(21)	1.313(10)	O(3)–C(15)	1.357(11)
C(7)–C(8)	1.321(14)	O(1)–W–Cl(1)	80.5(2)
O(1)–W–O(3)	81.5(2)	O(1)–W–Cl(2)	83.0(2)
O(3)–W–Cl(1)	161.9(2)	Cl(1)–W–Cl(2)	90.7(1)
O(3)–W–Cl(2)	85.9(2)	O(3)–W–Cl(3)	90.9(2)
O(1)–W–Cl(3)	80.3(2)	Cl(2)–W–Cl(3)	163.3(1)
Cl(1)–W–Cl(3)	87.4(1)	O(3)–W–C(7)	85.5(3)
O(1)–W–C(7)	158.5(3)	Cl(2)–W–C(7)	113.1(3)
Cl(1)–W–C(7)	113.1(3)	O(1)–W–C(8)	162.9(3)
Cl(3)–W–C(7)	82.9(3)	Cl(1)–W–C(8)	856.7(3)
O(3)–W–C(8)	111.8(3)	Cl(3)–W–C(8)	109.4(3)
Cl(2)–W–C(8)	87.0(3)	W–O(1)–C(21)	130.5(5)
C(7)–W–C(8)	38.3(4)	W–C(7)–C(1)	141.6(7)
W–O(3)–C(15)	136.7(5)	O(1)–C(21)–O(2)	119.6(8)
W–C(7)–C(8)	71.3(5)	W–C(8)–C(9)	144.1(7)
W–C(8)–C(7)	70.4(5)		

Table 2. Pertinent Bond Lengths (Å) and Angles (deg) for $W(\eta^2\text{-C}_2\text{Ph}_2)\text{Cl}_3(\text{Hcat}\cdots\text{OEt}_2)$

W–Cl(1)	2.363(3)	W–Cl(2)	2.362(3)
W–Cl(3)	2.367(3)	W–O(1)	2.240(7)
W–O(2)	1.942(7)	W–C(7)	2.006(10)
W–C(8)	2.014(9)	O(1)–C(15)	1.349(10)
C(7)–C(8)	1.315(15)	W–C(8)–C(7)	70.6(6)
O(2)–C(20)	1.356(9)	Cl(1)–W–Cl(3)	90.1(1)
Cl(1)–W–Cl(2)	163.7(1)	Cl(1)–W–O(1)	79.7(2)
Cl(2)–W–Cl(3)	86.2(1)	Cl(3)–W–O(1)	83.6(2)
Cl(2)–W–O(1)	84.1(2)	Cl(2)–W–O(2)	89.6(2)
Cl(1)–W–O(2)	88.3(2)	O(1)–W–O(2)	75.9(3)
Cl(3)–W–O(2)	159.4(2)	Cl(2)–W–C(7)	88.2(3)
Cl(1)–W–C(7)	107.5(3)	O(1)–W–C(7)	156.4(4)
Cl(3)–W–C(7)	118.1(3)	Cl(1)–W–C(8)	86.2(3)
O(2)–W–C(7)	81.8(4)	Cl(3)–W–C(8)	87.6(3)
Cl(2)–W–C(8)	109.5(3)	O(2)–W–C(8)	112.8(4)
O(1)–W–C(8)	163.3(4)	W–O(1)–C(15)	111.9(5)
C(7)–W–C(8)	38.2(4)	W–C(7)–C(6)	142.3(7)
W–O(2)–C(20)	120.1(5)	W–C(8)–C(14)	144.8(7)
W–C(7)–C(8)	71.3(6)		

seem different from the related distances in **1b** and **2**, but these bond lengths are also well within the range observed for isoelectronic $W(\eta^2\text{-R}_2\text{C}_2)$ and $\text{Mo}(\eta^2\text{-R}_2\text{C}_2)$ species.^{53–61} We might expect to see greater variations in bonding between the acetylene and tungsten when there are actual changes in the valence electron count at tungsten. There is an apparent trend toward lengthening of the $\text{C}\equiv\text{C}$ bonds in a pair of previously isolated d^3 and d^4 phosphine-substituted tungsten acetylene complexes, which could be explained by increasing back-donation into the π^* orbitals of the acetylene.⁶² But even in this case, it is not clear that the observed $\text{C}\equiv\text{C}$ distances are statistically different from those found in d^2 metal acetylene derivatives.

(55) Stahl, K.; Weller, F.; Dernicke, K. Z. *Anorg. Allg. Chem.* **1986**, *533*, 73.

(56) Kersting, M.; El-Kohli, A.; Miller, U.; Dehnicke, K. *Chem. Ber.* **1989**, *122*, 279.

(57) Pauls, R.; Dehnicke, K.; Fenske, D. *Chem. Ber.* **1989**, *122*, 481.

(58) Fenske, D.; Baum, G.; Hafacher, P.; Dehnicke, K. *Anorg. Allg. Chem.* **1990**, *585*, 27.

(59) Dierkes, P.; Dehnicke, K.; Fenske, D. *Z. Naturforsch.* **1994**, *49B*, 1391.

(60) Kersting, M.; Dehnicke, K.; Fenske, D. *J. Organomet. Chem.* **1986**, *309*, 125.

(61) Kersting, M.; Dehnicke, K.; Fenske, D. *J. Organomet. Chem.* **1988**, *346*, 201.

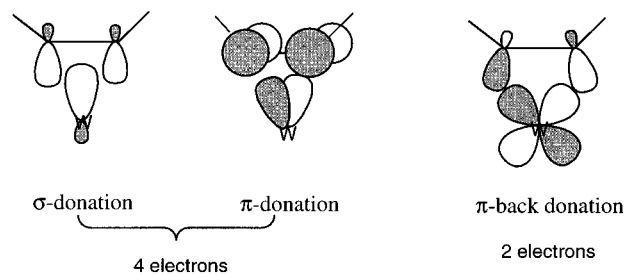
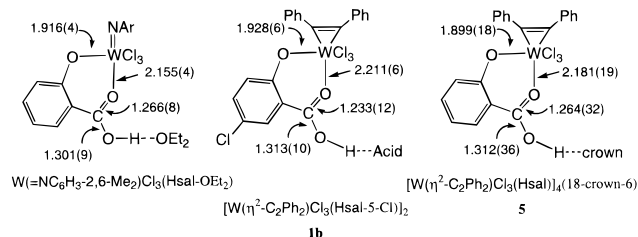
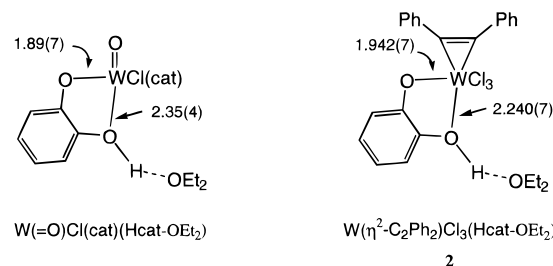
(62) Nielson, A. J.; Boyd, P. D. W.; Clark, G. R.; Hunt, P. A.; Hunsthouse, M. B.; Metson, J. B.; Richard, C. E. F.; Schwerdfeger, P. A. *J. Chem. Soc., Dalton Trans.* **1995**, 1153.

Table 3. Pertinent Bond Lengths (Å) and Angles (deg) for $[\text{W}(\eta^2\text{-C}_2\text{Ph}_2)\text{Cl}_3(\text{Hsal})_4 \cdots (18\text{-crown-6})]$

W(1)–Cl(1)	2.382(9)	W(2)–Cl(2)	2.321(8)
W(1)–Cl(3)	2.350(8)	W(1)–O(2)	2.166(19)
W(1)–O(3)	1.920(17)	W(1)–C(1)	2.053(26)
W(1)–C(2)	1.984(22)	W(2)–Cl(4)	2.359(7)
W(2)–Cl(5)	2.331(7)	W(2)–Cl(6)	2.372(7)
W(2)–O(5)	2.197(17)	W(2)–O(6)	1.895(18)
W(2)–C(4)	2.073(23)	W(2)–C(5)	2.012(20)
C(1)–C(2)	1.293(31)	C(4)–C(5)	1.238(36)
O(1)–C(37)	1.335(39)	O(2)–C(37)	1.240(32)
O(3)–C(36)	1.367(35)	O(4)–C(67)	1.261(28)
O(5)–C(67)	1.288(30)	O(6)–C(61)	1.424(28)
O(90)–C(90)	1.516(32)	O(90)–C(91)	1.392(34)
O(91)–C(92)	1.443(36)	O(91)–C(93)	1.399(27)
O(92)–C(94)	1.400(31)	O(92)–C(95)	1.378(38)
C(90)–C(95A)	1.594(43)	C(91)–C(92)	1.492(42)
C(93)–C(94)	1.532(38)	C(95)–C(90A)	1.594(43)

Cl(2)–W(1)–Cl(3)	90.5(3)	Cl(1)–W(1)–O(2)	80.5(5)
Cl(2)–W(1)–O(2)	82.0(5)	Cl(3)–W(1)–O(2)	82.0(5)
Cl(1)–W(1)–O(3)	91.5(6)	Cl(2)–W(1)–O(3)	163.4(6)
Cl(3)–W(1)–O(3)	86.2(6)	O(2)–(1)–O(3)	81.5(7)
Cl(1)–W(1)–C(1)	82.8(8)	Cl(2)–W(1)–C(1)	111.0(7)
Cl(3)–W(1)–C(1)	114.3(8)	O(2)–W(1)–C(1)	158.2(8)
O(3)–W(1)–C(1)	85.1(9)	Cl(1)–W(1)–C(2)	109.1(6)
Cl(2)–W(1)–C(2)	86.1(6)	Cl(3)–W(1)–C(2)	88.0(6)
O(2)–W(1)–C(2)	164.3(7)	O(3)–W(1)–C(2)	110.0(9)
C(1)–W(1)–C(2)	37.3(9)	Cl(4)–W(2)–Cl(5)	86.5(2)
Cl(4)–W(2)–Cl(6)	161.7(2)	Cl(5)–W(2)–Cl(6)	92.3(3)
Cl(4)–W(2)–O(5)	81.9(5)	Cl(5)–W(2)–O(5)	81.4(5)
Cl(6)–W(2)–O(5)	79.9(5)	Cl(4)–W(2)–O(6)	88.6(5)
Cl(5)–W(2)–O(6)	161.8(5)	Cl(6)–W(2)–O(6)	86.9(5)
O(5)–W(2)–O(6)	80.6(7)	Cl(4)–W(2)–C(4)	114.2(7)
Cl(5)–W(2)–C(4)	89.0(8)	Cl(6)–W(2)–C(4)	84.1(7)
O(5)–W(2)–C(4)	160.9(9)	O(6)–W(2)–C(4)	108.9(9)
Cl(4)–W(2)–C(5)	87.0(6)	Cl(5)–W(2)–C(5)	110.1(6)
Cl(6)–W(2)–C(5)	110.5(6)	O(5)–W(2)–C(5)	163.5(8)
O(6)–W(2)–C(5)	87.1(8)	C(4)–W(2)–C(5)	35.2(10)
W(1)–O(2)–C(37)	127.8(18)	W(1)–O(3)–C(36)	132.0(19)
W(2)–O(5)–C(67)	130.0(17)	W(2)–O(6)–C(61)	135.9(14)
W(1)–C(1)–C(2)	68.5(14)	W(1)–C(1)–C(16)	139.0(21)
C(2)–C(1)–C(16)	152.5(28)	W(1)–C(2)–C(1)	74.2(16)
W(1)–C(2)–C(26)	147.6(16)	C(1)–C(2)–C(26)	138.0(23)
O(2)–C(37)–C(35)	125.5(30)	W(2)–C(4)–C(5)	69.7(14)
W(2)–C(4)–C(46)	145.1(21)	C(5)–C(4)–C(46)	144.9(25)
W(2)–C(5)–C(4)	75.0(15)	W(2)–C(5)–C(56)	140.0(15)
C(90)–O(90)–C(91)	109.8(19)	C(92)–O(91)–C(93)	110.2(21)
C(94)–O(92)–C(95)	110.9(20)	O(90)–C(90)–C(95A)	103.3(19)
O(90)–C(91)–C(92)	109.2(21)	O(91)–C(92)–C(91)	108.9(27)
O(91)–C(93)–C(94)	108.5(21)	O(92)–C(94)–C(93)	109.5(20)
O(92)–C(95)–C(90A)	111.7(22)		

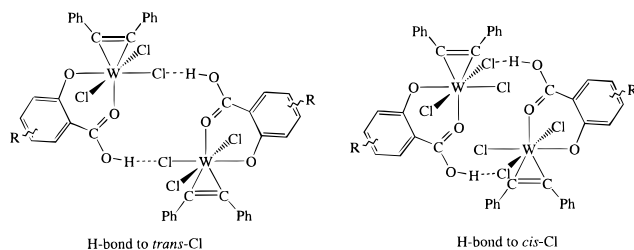
There has been ongoing discussion in the literature about the best bonding description for this class of mononuclear d^2 acetylene complexes.^{53,50,60–62} Some authors have claimed that the structural parameters of the tungsten derivatives provide little evidence for a true tungstacyclopropene-like valence structure.⁵³ Others, citing the extreme downfield shift of the acetylenic carbons, suggest that substantial positive charge resides on the acetylene carbons.⁵⁶ A more recent study likens the electronic structure of the d^2 acetylene complexes to that of a system bearing a d^0 tungsten arylimido unit.⁶² This latter description,⁶² based on careful structural, XPS, and calculational studies, seems most consistent with the observed chemistry of **1**. It should be noted, however, that the electronic structure of the acetylene ligand need not completely adopt the character of a stilbene dianion ($[\text{C}_2\text{Ph}_2]^{2-}$) in order to mimic the chemistry of an imido group. The most sensible simple model for bonding in the $\text{W}(\eta^2\text{-R}_2\text{C}_2)$ unit is one suggested by its ^{13}C NMR spectrum: a four electron donor acetylene ligand, which also acts as a two electron π back-acceptor from an occupied tungsten d orbital (Figure 5).⁶³ Consistent with this description, the

**Figure 5.** σ - and π -bonding scheme for a $\text{W}(\eta^2\text{-Ph}_2\text{C}_2)$ fragment.**Figure 6.** Detailed tungsten bond distances in angstroms (Å) for representative Hsal ligands.**Figure 7.** Detailed tungsten bond distances in angstroms (Å) for representative Hcat ligands.

coordination environment of the tungsten is a classic example of a d^0 octahedral complex that contains a single strong *trans* influence ligand.⁴¹ The square plane of the monoanionic ligands is bent an average of 9° away from the acetylene ligand, while the $\text{W}-\text{O}_{\text{COOH}}$ distance of 2.211(6) Å illustrates the *trans* influence of the Ph_2C_2 group.

Considering the potential electronic and steric influence of the acetylene unit, the core chelate structures of the Hsal and Hcat ligands are very similar in the $\text{W}(\eta^2\text{-R}_2\text{C}_2)\text{Cl}_3$ subunit and analogous oxo and arylimido complexes. Figures 6 and 7 compare the structures of Hsal-R and Hcat ligands in a variety of tungsten complexes.^{41,42} All of the Hsal-R and Hcat derivatives have long $\text{W}-\text{O}_{\text{Ph}}$ distances approximating 1.9 Å, characteristic of scant π -bonding between tungsten and the catecholate ligand. The three $\text{W}-\text{O}_{\text{COOH}}$ distances are also long, averaging 2.18(1) Å. Still, these distances are significantly shorter than the *trans* $\text{W}-\text{O}_{\text{OH}}$ distances 2.29(1) Å observed in the Hcat structures in Figure 7. The 0.11(1) Å difference between the *trans* $\text{W}-\text{O}_{\text{COOH}}$ and the *trans* $\text{W}-\text{O}_{\text{OH}}$ bond distance probably arises from two sources. First, and most significantly, the larger six-membered chelate of the Hsal ligand accommodates the coordination sphere of the tungsten better than the five-membered chelate of the Hcat group. Second, the sp^2 hybridization of the carboxylate oxygen probably contributes to a slightly shorter $\text{W}-\text{O}$ distance and a somewhat stronger $\text{W}-\text{O}$ bond. All of the Hcat

Scheme 1



and Hsal chelates remain virtually planar. The carboxylate units of the salicylate ligands all exhibit a localized valence bond structure, with the carbonyl oxygen bound to tungsten. None of the hydrogen-bonding interactions in **1b** and **5** manifest substantial carboxylate anion character, which may account for the roughly similar electronic distributions of the carboxylate units. Ammonium salts of these complexes can have much greater C–O bond delocalization in the acid functionality.⁴¹

Complex **1b** does not aggregate through a typical hydrogen-bonded acid dimer structure in the solid state but forms an enlarged ring in which the acid groups hydrogen bond to chloride ligands that are *cis* to the Hsal ligand on an adjacent molecule. The O–H...Cl distances are 3.03(2) Å, typical for solid-state O–H...Cl association.^{64,65} The *trans*-chloride ligand and the 5-chloro group play little role in the hydrogen bonding scheme, being approximately 3.3 and 5.6 Å away from the carboxylate oxygen, respectively. The “slippage” of these hydrogen bonding interactions from the classic acid dimer probably reflects both a reduction of electron density at the coordinated carbonyl unit and the greater steric congestion brought about by the neighboring metal center. The only apparent driving force for hydrogen bonding to the *cis*-chloride instead of the *trans*-chloride ligand is the collapse of the hydrogen-bonding ring into a more compact arrangement (Scheme 1). The hydrogen bonds are complemented by apparent vander Waals contacts between two $[W(\eta^2\text{-Ph}_2\text{C}_2)\text{Cl}_3(\text{Hsal})\cdots]_4$ (18-crown-6) units in which the Hsal-5-Cl ligand on one dimer stacks above the Hsal-5-Cl ligand of an adjacent dimer at a distance of 3.77(10) Å. Hydrogen bonding between the Hsal ligand and the 18-crown-6 molecule, and between the Hcat ligand and ether in **5** and **2**, respectively, is characteristic of the bonds found in other tungsten Brønsted acid adducts.^{22,23,28,41} Typical O...O distances found in these systems are 2.51(1) Å.

The ORTEP diagram of $[W(\eta^2\text{-Ph}_2\text{C}_2)\text{Cl}_3(\text{Hsal})\cdots]_4$ (18-crown-6) (**5**, Figure 4) is a representation of the most remarkable of these supramolecular aggregates. The 18-crown-6 molecule adopts a typical crown conformation, in which the acid moieties of the Hsal ligands hydrogen bond to four of the ether oxygens in a 1,4-, 10,13-substitution pattern. A large number of structures of the 18-crown-6 macrocycle exist, some of which hydrogen bond to water and small organic molecules.^{66–72}

(64) Hamilton, W. C. *Hydrogen Bonding in Solids*; W. A. Benjamin, Inc.: New York, 1968.

(65) For a related hydrogen bond interaction involving N–H...Cl bonds, see: Yap, G. P. A.; Rheingold, A. L.; Das, P.; Crabtree, R. H. *Inorg. Chem.* **1995**, *34*, 3474.

(66) Watson, K. A.; Fortier, S.; Murchie, M. P.; Bovenkamp, J. W.; Rodriguez, A.; Buchanan, G. W.; Ratcliffe, C. I. *Can. J. Chem.* **1990**, *68*, 1201.

Typically, in structures of non-hydrogen-bonded and non-metal-coordinated 18-crown-6 molecules, dihedrals are observed to be 60° around the C–C bonds and 180° around the C–O bonds.^{73,74} This lends the macrocycle its characteristic shape with the oxygen atoms oriented toward the interior of the structure. This orientation is largely maintained in the $[W(\eta^2\text{-Ph}_2\text{C}_2)\text{Cl}_3(\text{Hsal})\cdots]_4$ (18-crown-6) complex, in which all of the atoms in the 18-crown-6 show a 0.248(40) Å RMS deviation from planarity. Like the hydrogen bonds in hydrates, chloroform, and chloroacetonitrile adducts of 18-crown-6,^{67,68,71,72} the hydrogen-bonding interactions in **5** are not bifurcated but exhibit standard O...O distances averaging 2.51(1) Å. The hydrogen-bonding interactions pull the ether oxygens slightly farther than normal out of the interior of the ring, which may be responsible for the slight observed increase in the O–C–C–O torsional angles to 64.1° (average). The juxtaposed O(90), O(90') oxygens, which are free of hydrogen bonding, seem to be protected from coordination to additional equivalents of free acid by the steric demands of the proximate tungsten centers. These oxygens come closest to the achieving the gauche O–C–C–O dihedrals (62.2°) expected for a noninteracting 18-crown-6 molecule. The carboxylate moiety of the Hsal subunit π -stacks above the aromatic ring of the Hsal subunit on the cofacial tungsten complex with an inter-arene plane distance of 3.39(18) Å. This “sandwiches” the non-hydrogen-bonded ether oxygens between adjacent $W(\eta^2\text{-Ph}_2\text{C}_2)\text{Cl}_3(\text{Hsal})$ molecules, providing the steric protection noted above. Similar steric congestion evidently also occurs in the d⁰ oxo and arylimido analogs, which are isolated with identical tetranuclear stoichiometries.⁴¹

Conclusions. Approaches to constructing materials with novel structural and chemical behavior can further our understanding of basic concepts such as hydrogen bonding. The organometallic free acids described in this study provide an unusual opportunity for a detailed study of how subtle steric and electronic perturbations in ligand sets influence the reactivity and hydrogen bonding ability of high oxidation state early transition metal Brønsted acids. The study of these complexes fosters the development of other applications intimately related to hydrogen bonding, such as molecular recognition and the preparation of novel inorganic/organic hybrid materials.

Experimental Section

General Procedures and Materials. All experiments were performed under a nitrogen atmosphere in a HE-553-2 Vacuum Atmospheres drybox or using standard Schlenk techniques. Hexane and diethyl ether were purified by distil-

(67) Mootz, D.; Albert, A.; Schaeffgen, S.; Stäber, D. *J. Am. Chem. Soc.* **1994**, *116*, 12045.

(68) Strel'tsova, W. R.; Bel'skii, Y. K.; Nazarenko, A. Y.; Kranifovski, O. T. *Z. Obshch. Khim.* **1992**, *62*, 598.

(69) Blaschette, A.; Safari, F.; Nagel, K.; Jones, P. G. *Z. Naturforsch.* **1993**, *1355*.

(70) Audet, P. J.; Savoie, R.; Simard, M. *Can. J. Chem.* **1990**, *68*, 2183.

(71) Jones, P. G.; Hiemisch, O.; Blaschette, A. *Z. Naturforsch.* **1994**, *852*.

(72) Buchanan, G. W.; Rodrigue, A.; Bensimon, C.; Ratcliffe, C. I. *Can. J. Chem.* **1992**, *70*, 1033.

(73) Miele, P.; Foulton, J.; Hovnanian, N.; Cot, L. *Polyhedron* **1993**, *12*, 267.

(74) Dunitz, J. D.; Dobler, M.; Seiler, P.; Phizackerley, R. P. *Acta Crystallogr., Sect. B* **1974**, *30*, 2733.

lation from Na/benzophenone. Dichloromethane, acetonitrile, and triethylamine were purified by distillation from CaH₂, followed by degassing with dry nitrogen. NMR solvents (Cambridge Isotope Laboratories) were dried with 5 Å molecular sieves and degassed with dry nitrogen. Celite was oven dried for 48 h at 110 °C prior to use. Salicylic acid (H₂sal, Fisher), substituted salicylic acids (H₂sal-R, Aldrich), and diphenylacetylene (Ph₂C₂, Farchan) were used as received. 18-Crown-6 was recrystallized from dry acetonitrile and vacuum dried for 12 h (~10⁻⁶ Torr, room temperature) prior to use. W(η²-Ph₂C₂)Cl₄ was synthesized from sublimed WCl₆ and Ph₂C₂ according to literature procedures.⁴⁴

NMR spectra were recorded on Varian XL-300, GE QE-300, or Bruker AM-500 spectrometers. ¹H and ¹³C data are listed in parts per million downfield from tetramethylsilane, with data referenced by the residual solvent proton peak. Elemental analyses were performed by Desert Analytics (P.O. Box 41838, Tucson, AZ 85717).

Preparation W(η²-Ph₂C₂)Cl₃(Hsal) (1a). W(η²-Ph₂C₂)Cl₄ (4.496 g, 8.92 mmol) was slurried in 25 mL of CH₂Cl₂ and 15 mL of hexane in a 50 mL Schlenk flask. To this reddish-purple slurry, salicylic acid (1.231 g, 8.91 mmol) was added by addition tube. The mixture immediately darkened to a deep orange-red color. The flask was fitted with a condenser and refluxed for 6 h. A brick red, microcrystalline powder precipitated and was harvested via filtration. The precipitate was washed with hexane (2 × 15 mL) and dried for 8 h (~10⁻⁶ Torr, room temperature). Yield: 4.061 g (75%). NMR data (CDCl₃) are as follow. ¹H: 6.95 (1H, d, 3-position Hsal), 7.29 (1H, t, 4-position Hsal), 7.58 (2H, t, 4-position of Ph- in Ph₂C₂), 7.74 (5H, t, overlapping protons of 5-position on salicylate and 3-position of Ph- ring on the Ph₂C₂ ligand), 8.14 (4H, d, 2-position of Ph- in Ph₂C₂), 8.27 (1H, d, 6-position Hsal). ¹³C: 112.47, 121.73, 125.11, 129.16, 132.47, 133.60, 134.49, 138.48, 138.93, 163.75, 165.64, 248.40 (Ph₂C₂). Analytical data are based on the formula C₂₁H₁₅O₃WCl₃. Calc: 41.65, C; 2.50, H. Actual: 41.51, C; 2.30, H.

Preparation of W(η²-Ph₂C₂)Cl₃(Hsal-5-Cl) (1b). A weighed portion of W(η²-Ph₂C₂)Cl₄ (0.7766 g, 1.54 mmol) and a stir bar were placed in a 50 mL Schlenk flask and then suspended in ~30 mL of dichloromethane. 5-Chlorosalicylic acid (0.2660 g, 1.54 mmol) was added by addition tube. Again, the color of the solution changed to a deep red-orange. The reaction was allowed to stir overnight and was then filtered through Celite. The volume was reduced *in vacuo* to 10 mL and then 5 mL of hexane was added. The solution was warmed and allowed to stand overnight yielding reddish block crystals suitable for X-ray analysis. Yield: 0.635 g (64%). NMR data (300 MHz, CDCl₃) are as follow. ¹H: 6.88 (H, d), 7.59 (2H, t), 7.64 (H, d), 7.67 (H, d), 7.74 (4H, t), 8.12 (4H, d), 8.21 (2H, d, *J*_m = 2.6 Hz). ¹³C: 113.32, 123.47, 129.24, 130.07, 131.65, 133.83, 134.56, 138.42, 138.85, 162.60, 170.25, 249.77 (Ph₂C₂).

Preparation of W(η²-Ph₂C₂)Cl₃(Hcat-Et₂O) (2). Catechol (0.218 g, 1.98 mmol) was dissolved in 20 mL of Et₂O and added to a solution of W(η²-Ph₂C₂)Cl₄ (1.00 g, 1.98 mmol) in 15 mL of Et₂O. The dark reddish-purple solution was stirred overnight and then filtered through Celite. The resulting solution was reduced in volume to ~5 mL and cooled to -20 °C to afford purple block crystals suitable for X-ray analysis (1.05 g, 1.61 mmol, 81%). NMR data (500 MHz, CDCl₃) are as follow. ¹H: 1.46 (6H, t, (CH₃CH₂)₂O), 3.90 (4H, q, (CH₃CH₂)₂O), 6.99 (H, d), 7.07 (H, t), 7.12 (H, t), 7.27 (H, d), 7.59 (2H, t), 7.73 (4H, t), 8.24 (4H, d), 14.97 (H, broad s, Hcat-Et₂O). ¹³C: 14.85, 67.44, 114.84, 118.50, 123.17, 126.29, 129.07, 133.44, 134.44, 138.11, 144.68, 156.12, 247.14 (η²-Ph₂C₂). Analytical data are based on the formula C₂₄H₂₅O₃WCl₃·1/3C₄H₁₀O. Calc: 44.98, C; 4.21, H. Actual: 45.45, C; 3.83, H.

Preparation of *cis*-W(η²-Ph₂C₂)Cl₂(edbp)(OEt₂) (3). A weighed portion of W(η²-Ph₂C₂)Cl₄ (0.488 g, 0.968 mmol) and a stir bar were placed in a 50 mL Schlenk flask and then

suspended in toluene (10 mL). LiHedbp (0.502 g, 0.968 mmol where edbp = 2,2'-ethylenebis(4,6-di-*tert*-butylphenolate)) dissolved in ether (20 mL) was added via cannula. The reaction was refluxed overnight, yielding a dark red solution and a light colored precipitate. After filtration through Celite, and a second filtration in ether/hexane solution, the filtrate volume was reduced. Refrigeration at -20 °C yielded a black microcrystalline solid of *cis*-W(η²-Ph₂C₂)Cl₂(edbp)(OEt₂) (3). Yield: 0.291 g (0.32 mmol, 33%). The product was prone to loss of ether. NMR data (300 MHz, CDCl₃) are as follow. ¹H: 8.30 (d, 4H, Ph₂C₂), 7.65 (t, 4H, Ph₂C₂), 7.56 (s, 1H, Ph₂C₂), 7.38 (s, 2H, edbp), 7.24 (s, 2H, edbp), 4.13 (q, 1H, CHCH₃, edbp), 3.48 (q, 4H, OCH₂CH₃), 2.12 (d, 3H, CHCH₃, edbp), 1.34 (s, 18H, C(CH₃)₃), 1.03 (s, 18H, C(CH₃)₃). ¹³C: 227.62 (Ph₂C₂), 161.42, 150.14, 147.30, 142.94, 141.11, 135.95, 133.82, 132.76, 130.00, 128.84, 123.21, 122.53, 121.95, 120.73, 65.86 (CH₃CH), 31.62 (C(CH₃)₃), 31.51 (C(CH₃)₃), 15.27 (CH₃CH).

Preparation of W(η²-Ph₂C₂)Cl₃(Hsal)···NEt₃ (4a). **1a** (0.899 g, 1.48 mmol) was placed into a 50 mL Schlenk flask and slurried in 15 mL of benzene. Triethylamine (0.21 mL, 0.152 g, 1.50 mmol) was added by syringe over 5 min. The solution darkened as the triethylamine was added and was then allowed to stir for 30 min. The resulting orange-red mixture was stripped to dryness, yielding a spongy mass that dried further under high vacuum. Hexane (40 mL) was added to the flask, and the solid mass was broken up with agitation. The suspension was filtered, leaving orange-red microcrystals that were washed with hexane (2 × 10 mL) and dried for 3 h *in vacuo*. Yield: 0.943 g (1.33 mmol, 90%). NMR data (300 MHz, CDCl₃) are as follow. ¹H: 1.40 (9H, t), 3.35 (6H, m), 6.77 (H, d), 7.16 (H, t), 7.44 (H, t), 7.49 (2H, t, overlaps w/peak at 7.44 ppm), 7.67 (4H, t), 8.15 (4H, d), 8.26 (H, d), 11.70 (H, br s, -CO₂H···NEt₃). ¹³C: 9.08 (N(CH₂CH₃)₃), 46.03 (N(CH₂-CH₃)₃), 119.56, 120.68, 125.01, 128.85, 132.25, 132.31, 133.71, 134.08, 140.24, 162.70, 169.58, 244.95 (Ph₂C₂). Analytical data are based on the formula C₂₁H₃₁N₃O₃WCl₃. Calc: 45.91, C; 4.28, H; 1.98, N. Actual: 46.16, C; 4.13, H; 1.83, N.

Preparation of [W(η²-Ph₂C₂)Cl₃(Hsal)···]₄(18-crown-6) (5). This experiment was carried out in a fashion similar to the synthesis of **1a** or **1b** with 18-crown-6 present. A 50 mL Schlenk flask was charged with W(η²-Ph₂C₂)Cl₄ (2.6760 g, 5.31 mmol) and a stir bar. In a separate flask, salicylic acid (0.7345 g, 5.32 mmol), 18-crown-6 (0.2393 g, 0.90 mmol), and ~40 mL of dichloromethane were combined. This solution was transferred, by cannula, to the Schlenk flask containing the solid W(η²-Ph₂C₂)Cl₄. Before all of the solution was transferred, all of the tungsten-containing materials had dissolved. This red-brown solution was stirred overnight and then filtered through Celite. The volume of solution was reduced to ~20 mL, and then the flask was closed and cooled at -20 °C, yielding X-ray-quality orange-red block crystals. The supernatant solution yielded further crops of crystals after further reduction in volume and layering with hexane. Yield: 2.175 g (3.42 mmol, 61%). NMR data (300 MHz, CDCl₃) are as follow. ¹H: 4.10 (24H, s), 6.86 (4H, d), 7.18 (4H, t), 7.56 and 7.62 (12H, overlapping triplets), 7.72 (16H, t), 8.14 (16H, d), 8.25 (4H, d), 11.8 (4H, broad s, -COOH···OCH₂-). ¹³C: 70.89, 113.37, 121.39, 125.15, 129.08, 132.57, 133.33, 134.42, 138.06, 138.67, 163.39, 171.58, 247.47 (Ph₂C₂). Analytical data are based on the formula C₉₆H₈₄O₁₈W₄Cl₁₂. Calc: 42.92, C; 3.15, H. Actual: 43.17, C; 3.00, H.

Molecular Weights of Free Acids. The molecular weights of the free acids in benzene solution were determined using a modified Signer apparatus.⁴⁸ The apparatus makes use of the property of the change in vapor pressure of a solvent as a function of concentration of solute (i.e. Raoult's Law). A standard solution of triphenylmethane was placed in one side of the apparatus and the complex solution placed in the other. The apparatus was then sealed (using Kontes Teflon valves), and the volume of each solution is measured. When the volume of the two solutions stopped changing, the vapor

Table 4. Crystallographic Data for **1b**, **2**, and **5**

	1b	2	5
(a) Crystal Parameters			
formula	C ₂₁ H ₁₄ Cl ₄ O ₃ W	C ₂₄ H ₂₅ Cl ₃ O ₃ W	C ₉₆ H ₈₄ Cl ₁₂ O ₁₈ W ₄
fw	640.0	651.6	2686.5
cryst system	triclinic	monoclinic	triclinic
space group	$P\bar{1}$	$P2_1/n$	$P\bar{1}$
<i>a</i> , Å	10.009(3)	9.396(4)	10.682(3)
<i>b</i> , Å	10.725(3)	24.849(6)	12.201(3)
<i>c</i> , Å	10.796(3)	10.932(5)	19.244(3)
α , deg	105.70(2)		81.70(3)
β , deg	97.84(2)	95.35(3)	76.77(5)
γ , deg	92.02(2)		85.66(3)
<i>V</i> , Å ³	1102.0(2)	2544(4)	2416(6)
<i>Z</i>	2	4	1
cryst dimens, mm	0.40 × 0.40 × 0.30	0.38 × 0.42 × 0.46	0.32 × 0.34 × 0.36
cryst color	red	black	black
<i>D</i> (calc), g cm ³	1.928	1.701	1.892
Mo K α , cm ⁻¹	57.45	48.78	51.55
temp, K	228	296	296
<i>T</i> (max)/ <i>T</i> (min)	0.62/0.41	0.88/0.62	0.57/0.32
(b) Data Collection			
diffractometer		Siemens P4	
monochromator		graphite	
radiation		Mo K α (λ = 0.710 73 Å)	
2 θ scan range, deg	4–48	4–50	4–44
rflns colld	3678	4688	6120
indepd rflns	3011	4449	5905
indepd obsd reflns $F > n\sigma(F_o)$	3011 ($n = 4$)	2840 ($n = 4$)	3942 ($n = 4$)
stds/reflcs	3 stds/197 rflns	3 stds/197 rflns	3 stds/197 rflns
var in stds, %	<1	1–2	<1
(c) Refinement ^a			
<i>R</i> (<i>F</i>), %	4.24 (4.98) ^b	4.04 (7.75)	7.42 (11.00)
<i>R</i> (<i>wF</i>), %	5.20 (5.37) ^b	4.70 (5.68)	10.27 (11.86)
$\Delta\sigma$ (max)	0.010	0.129	0.043
$\Delta(\rho)$, e Å ⁻³	1.89	0.65	1.59
<i>N</i> _o / <i>N</i> _v	11.5	11.6	10.2
goodness of fit	1.21	1.00	1.18

^a Quantity minimized = $\sum w\Delta^2$; $R = \sum \Delta / \sum (F_o)$; $R(w) = \sum \Delta w^{1/2} / \sum (F_o w^{1/2})$, $\Delta = |(F_o - F_c)|$. ^b All data.

pressures were assumed to have equalized and the molecular weight was calculated.

¹H NMR Titration of **1b** with Triethylamine in CDCl₃.

A 4.35 mg amount of **1b** was weighed directly into a calibrated NMR tube, dissolved in CDCl₃, and diluted to a total volume of 750 μ L. The tube was capped with a septum and secured with Parafilm. Triethylamine (0.102 g) was placed into a 1 mL volumetric flask and was subsequently diluted to the mark with CDCl₃. This flask was also capped with a septum and secured with Parafilm. Triethylamine solution (1 μ L aliquots, 1.01 M) was added to the solution containing **1b** (1.10×10^{-2} M) via microliter syringe and then allowed to equilibrate for 1 min. NMR spectra were recorded at 20 °C. At high triethylamine concentrations, only one broad peak is observed, attributed to fast exchange of the salt **4b** with the free acid **1b** remaining.

Crystallographic Structure Determinations. Crystallographic data are collected in Table 4. Specimens of all three compounds were mounted on glass fibers and characterized photographically. Structures **1b** and **5** showed no symmetry greater than triclinic, and **2** was found to possess $2/m$ Laue symmetry. For **1b** and **5** an initial assumption of centrosymmetry was supported by the results of the subsequent refinement; for **2** the space group was uniquely determined by systematic absences. Empirical corrections for absorption were applied to the data. All structures were solved from

Patterson syntheses. All non-hydrogen atoms were refined with anisotropic thermal parameters, except for the phenyl-ring carbon atoms of **5** which were refined isotropically to conserve data. Hydrogen atoms are treated as idealized contributions. The nonrigidity of the loosely-bound crown ether complex produces higher-than-usual thermal activity that, in turn, creates diffuse diffraction. *R* factors and other measures of structure quality compare favorably to those commonly reported for similar compounds. All computations used SHELX software (version 4.2, G. Sheldrick, Siemens XRD, Madison, WI).

Acknowledgment. We gratefully acknowledge the Petroleum Research Fund, administered by the American Chemical Society, for support of this research. We also thank Hercules Corp. for a generous gift of tungsten compounds and a drybox in support of this work.

Supporting Information Available: Tables of atomic coordinates and *U* values, interatomic distances, angles, and anisotropic displacement coefficients and supplementary views of inter-arene contacts (39 pages). Ordering information is given on any current masthead page.

OM960361G